Indian Journal of Engineering & Materials Sciences
Vol. 31, October 2024, pp. 721-727
DOI: 10.56042/ijems.v31i5.11234

Development and analysis of zeolite-based electrodes drived from fly ash for supercapacitor application

Vinay Kumar[a*], Rita Dahiya[a], Suman Rani[a], Sunil Kumar[a], Anushree Jatrana[b]& Nitin Bhardwaj[c]

[a]Department of Physics, CCS Haryana Agricultural University, Hisar, Haryana 125 004, India

[b]Department of Chemistry, CCS Haryana Agricultural University, Hisar, Haryana 125 004, India

[c]Department of Agronomy, COA, CCS Haryana Agricultural University, Hisar, Haryana 125 004, India

Received: 18 May 2024; accepted: 22 September 2024

In the current global scenario, the pressing challenges of energy scarcity and environmental degradation profoundly impact the pursuit of sustainable development. The present study involved the preparation of zeolite by utilizing waste material (fly ash) obtained from a thermal power plant. An easy and cost-effective method for utilizing waste to generate useful material has been provided by hydrothermal crystallization for the preparation of zeolite. To analyze the as-synthesized material, X-ray diffraction (XRD), Fourier transform infrared (FTIR) spectroscopy, Field emission scanning electron microscopy (FE-SEM), and Brunauer-Emmett-Teller (BET) analysis have been used. The electrochemical investigation of as prepared material illustrates excellent capacitive behavior and shows a specific capacitance of 25 Fg^{-1} at 0.5 Ag^{-1} with an unprecedented specific surface area of 118.812 m^2g^{-1}.This study reveals the pathway of waste management in the direction of developing energy harvesting material.

Keywords: Fly ash, Hydrothermal crystallization, Porous, Electrode, Waste management

1 Introduction

In the present global scenario, the critical challenges of the energy crisis and environmental degradation have significantly influenced the trajectory of sustainable development. In India, the cornerstone of electricity production rests upon thermal power plants, predominantly fueled by coal. Subsequently, hydroelectric, nuclear, gas and diesel-powered plants play integral roles, collectively contributing to the diverse energy landscape of the nation[1]. Coal-based thermal power plants account for 75% of the total electricity generated[2]. In India, there are 155 such plants with a combined installed capacity of 157,377.00 MW. These plants consume 509.46 million tonnes (MT) of coal and produce 169.25 MT of fly ash. Since most power plants in the world run on coal, fly ash production has become the greatest industrial waste produced worldwide. Only 69% of the fly ash is used; the remaining ash is disposed of on disposal land, where it is exposed to various environmental conditions[3,4].Given that fly ash in landfills should be a possible source of hazardous materials entering groundwater and soil, as well as additional possible hazards to human health and the environment, a lot of study is going on to find ways to use fly ash in many industries[5].Numerous researchhas been carried out to determine the most prominent way to use fly ash and to comprehend the possible negative effects that landfilling may have on the environment and human health[4]. One of the solutions is to produce zeolite from fly ash. The primary components of fly ash are certain oxides (SiO_2 and Al_2O_3) that are left over after coal is burned and are formed from inorganic molecules that help in the formation of zeolite[6].Thus, it is anticipated that turning coal fly ash into zeolite will at least partially address the issue of fly ash disposal and so reduce its environmental impact[7]. Zeolites, intricate crystalline structures composed of hydrated aluminosilicate compounds, exhibit well-defined nanopores endowed with exceptional thermal, mechanical, chemical, and high-pressure resilience. Among the diverse spectrum of zeolite variants, NaP stands out as an intriguingly structured type, characterized by its intersecting channels and profound catalytic properties[8]. Their distinctive tetrahedral structure, which is organized in linked rings to produce micropores, is well known. These micropores provide a high specific surface area and high ion exchange capacity, two qualities that are necessary for electrode material to be employed in

*Corresponding author: (E-mail: vinay23@hau.ac.in)

supercapacitors[9]. An electrochemical device that stores energy is a supercapacitor[10]. Charge storage capacitors (SCs) fall into two types based on the fundamental principles of charge storage systems: electric double-layer capacitors (EDLC) and pseudo capacitors. The charge will be electrostatically stored in the non-faradaic double-layer in EDLC. Pseudocapacitors are devices that faradically store the charge generated by redox processes[11]. The present study explored the preparation of fly ash-derived Na-P zeolite as electrode materials for supercapacitors. Fly ash is converted into zeolite by simple hydrothermal crystallization method. This cost-effective and synergistic approach facilitates the utilization of fly ash as a material for electrochemical energy storage, offering a novel avenue for the eco-friendly utilization of solid waste.

2 Materials and Methods

2.1 Pre-treatment of fly ash

The chemical reagent used during whole process are HCl(37% (w/w), Loba Chemie), sodium hydroxide pellet(Purity 98%, Loba chemie), carbon black (Loba chemie), polyvinylidene fluoride (sigma) and N-Methyl-2- pyrrolidine(Purity 98%, Qualigens).The fly ash (FA) was initially screened to remove large-size particles and oven-dried at 105ºC. To eliminate the unburned carbon, the dried samples were afterwards calcined for two hours at 650ºC in a muffle furnace. Additionally, the obtained samples underwent treatment with HCl (10% v/v)for 5 hours at 85ºC in a hot air oven to remove other impurities. Then it was filtered and washed with double distilled water to get rid of all adulterations and neutralize pH. Finally, the material dried in an oven at 105ºC.

2.2 Hydrothermal crystallization

For this 5g of fly ash was treated with 30 mL of 2M NaOH solution at 85ºC for 48 hours under magnetic stirring at 500 rpm using reflux method. After centrifugation of the solution, the sample was washed with double distilled water to attain a neutral pH. The final product was oven-dried at 105ºC for overnight. The dried sample was subjected to further analysis. Fig. 1 illustrates the schematic representations of the whole synthesis process.

3 Results and Discussion

3.1 X-ray diffraction (XRD)

The XRD spectra of the synthesized zeolite is depicted in Fig. 2(a). The diffraction angle (2θ) ranged from 10º to 60º, assisting in the determination of the crystal structure of the synthesized zeolite. The XRD patterns elucidate that the hydrothermal synthesis of zeolite from fly ash in an alkaline

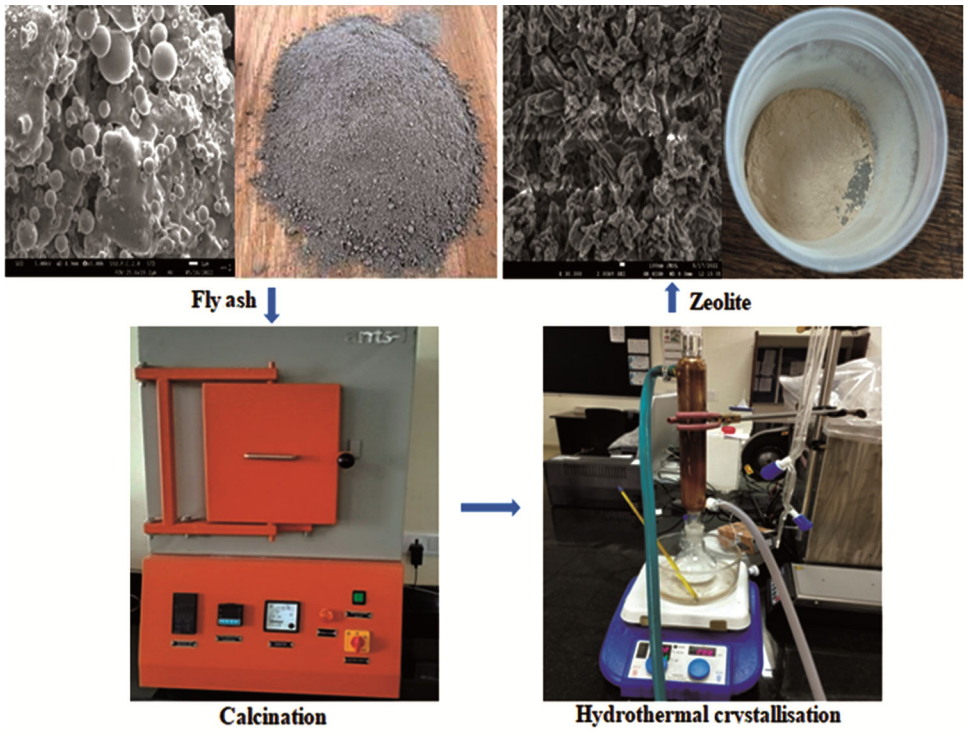

Fig. 1 — Schematic representation of synthesis process for Zeolite.

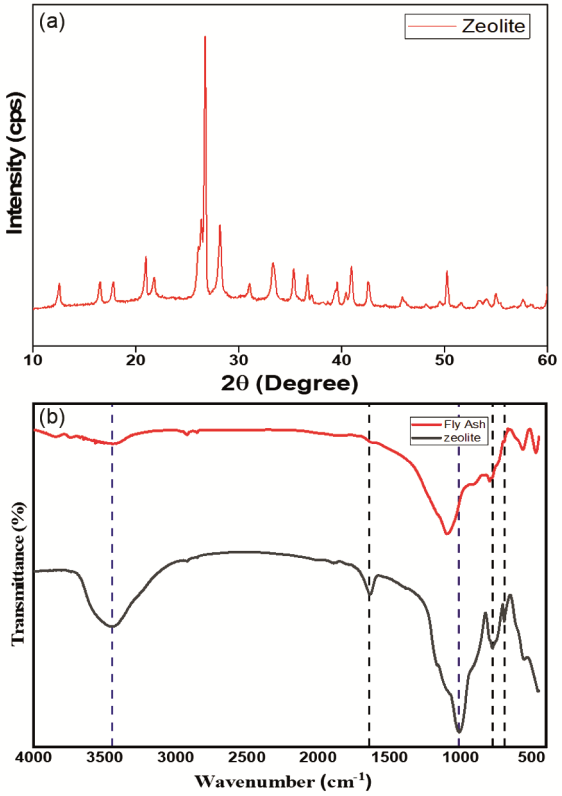

Fig. 2 — (a) XRD of zeolite and (b) FTIR spectra of zeolite and fly ash.

medium leads to the alteration of fly ash into zeolite P, along with the formation of a more stable crystalline phase of sodalite. Additionally, the presence of the quartz phase is detected in the final product. The sharp peaks observed in the XRD patterns signify the excellent crystallinity of the material. Furthermore, the crystallite size (D) of the zeolite was determined by Debye Scherrer formula using equation (1) and the D value of the zeolite is calculated to be 22.3 nm.

$$D = \frac{k\lambda}{\beta\cos\theta} \quad \ldots (1)$$

The symbols denote their usual meanings, i.e. kshape factor (constant value of 0.9), λ wavelength of the X-rays, βfull-width half maximum (FWHM) and θ diffraction angle.

3.2 Fourier Transform Infrared (FTIR) Spectroscopy

The FTIR spectra of both FA and zeolite are depicted in Fig. 2(b). The analysis of functional groups present in both materials was conducted using an FTIR spectrometer. In Fig. 2(b), a sharp and narrow band within the 1200-950 cm^{-1} range is observed, which is credited to the internal tetrahedral vibrations of Si-O-Si and Si-O-Al bonds. Specifically, in the zeolite, this band is observed at approximately 1010.91 cm^{-1}. This characteristic peak directs the presence of specific bonds within the structure of the zeolite, suggesting a successful transformation from raw fly ash to zeolite. When the concentration of Al atoms in the framework of tetrahedral sites increased, this vibration band changed towards a lower wave number, which was important for estimating the concentration of Al atoms in the crystalline framework. Furthermore, the force constant for the vibrational mode in an Al–O–Si bond is lower than the similar mode in a Si–O–Si linkage. This is because the replacement of Al^{3+} for Si^{4+} results in a longer Al–O bond, which lowers the T–O–T angle and lowers the frequency[12]. As a result, the bands in the raw fly ash at around 1090 cm^{-1} sharpened and moved to a lower frequency in the final product, indicating that the fly ash's vitreous components generate zeolitic material by reacting with the alkaline activator (NaOH)[13]. In addition, the vibration due to the presence of water molecules bonded to the zeolite framework produces distinctive bands given by bending vibrations at 1640 $cm^{-1}$and at 3450.42 cm^{-1}. Furthermore, the symmetric stretching of the Si-O-Si and Si-O-Al bonds is shown by the bands at 772.94 cm^{-1} and 689.54 cm^{-1}respectively[6].

3.3 UV-Visspectroscopy

In Fig. 3(a), the spectra of the synthesized zeolite reveal an adsorption peak at 300 nm.The band gap of synthesized material has been calculated using the Tauc plot method, shown in Fig. 3(b) and found to be 3.35 eV.

3.4 Brunauer-Emmett-Teller (BET) analysis

The N_2 adsorption-desorption isotherms of the pre-treated fly ash and the zeolite is shown in Fig. 4(a) and (b) respectively. The surface area of fly ash is found to be 3.007 m^2g^{-1} while the zeolite has a much higher surface area of 118.812 m^2g^{-1} following the BET method. The adsorption-desorption isotherms match the type IV classification[14], which specifies the typical mesoporous structure of zeolite. Based on the IUPAC classification, hysteresis loops observed within the relative pressure range of 0.45 to 0.95 are classified as type H3, signifying the mesoporous structure of the material as prepared[15].

3.5 Field Emission Scanning Electron Microscopy (FE-SEM)

The micrographs of fly ash and the as-prepared zeolite at different scales and magnifications are displayed in Fig. 5(a, b and c) and Fig. 5(d, e, f and g)

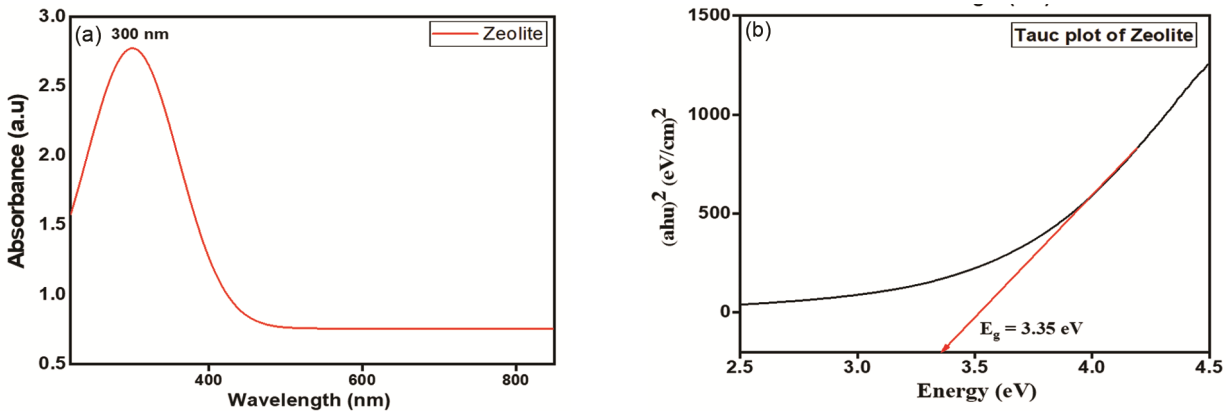

Fig. 3 — (a) UV-Vis spectra of zeolite, (b) Tauc plot of zeolite.

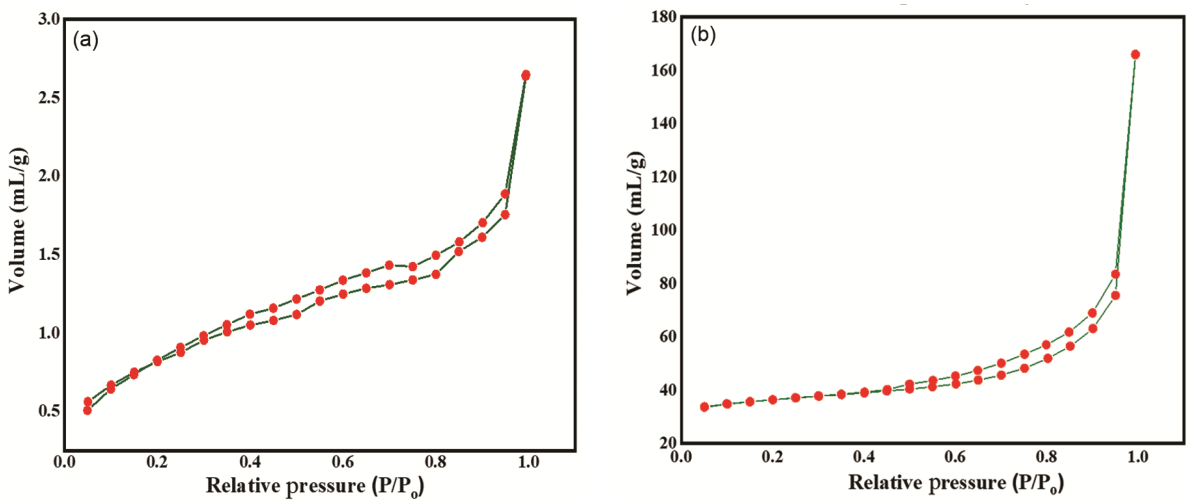

Fig. 4 — N_2 adsorption-desorption isotherms of pre-treated (a) fly ash, and (b) the synthesized zeolite.

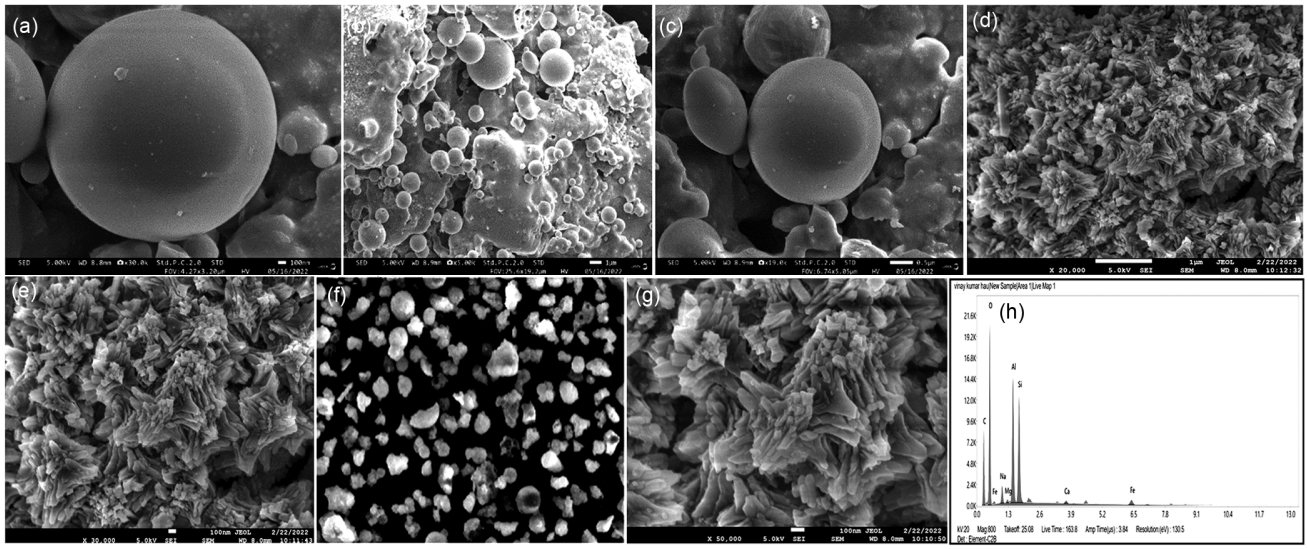

Fig. 5 — FE-SEM images of (a, b, c) fly ash, (d, e, f, g) synthesized zeolite at different magnifications, and (h) EDS spectrum of zeolite.

respectively. These images clearly shows that the zeolite is grown outside the surface of the fly ash and also confirm that zeolite has a larger surface area than the fly ash. The mesoporous structures are visible in the images of zeolite.

The hydrothermal treatment of fly ash results in a crystalline structure typical for zeolite P. Zeolite P aggregates with a lamellar and acicular morphology were observed.

The analysis of the chemical composition of zeolite shown by EDS spectra is represented by Fig. 5(h) which proves that the main elements present are C, O, Si, Al and Na. The elemental concentration of synthesized zeolite is presented in Table 1. The Si to Al ratio for the synthesized zeolite is found to be 0.8.

3.6 Electrochemical analysis zeolite electrode

3.6.1 Preparation of electrode

The mixture of Zeolite (16 mg), carbon black (2 mg) and binder polyvinylidene fluoride (2mg), was put in "N-Methyl-2- pyrrolidine (2 mL)" and stirred at a magnetic stirrer for 12 hours to form a uniform thick mixture. The resulting thick slurry was pasted on a graphite sheet with a mass loading of 1 mg and oven-dried in a vacuum oven at 80ºC over night as displayed in Fig. 6. The three-electrode setup i.e. working (synthesized material based), reference (Ag/AgCl) and counter (spiral platinum wire) electrodes were used for the electrochemical analysis.

Table 1— Elemental *c*omposition of zeolite.

Element	C	O	Na	Mg	Al	Si	Ca	Fe
Weight (%)	45.4	43.1	1.5	0.2	4.9	3.9	0.2	0.8

Using Equation (2), the specific capacitance was determined through the analysis of the galvanostatic charging-discharging (GCD).

$$C_s = \frac{I \times t}{m \times \Delta V} \quad \ldots (2)$$

The symbols denote their usual meanings, i.e. C_s specific capacitance (F g^{-1}), I discharge current (A), t discharging time(s), m mass loaded on the electrode (g), ΔV potential window (V).

3.6.2 Cyclic Voltammetry (CV)

The CV was used to investigate the ability of charge storage of prepared zeolite. The voltage window of 0.0 to 1.0 V was chosen owing to the best electrochemical performance of the electrode. The CV curves of zeolite at different scan rates ranging from 10 to 100 $mVs^{-1}$are depicted in Fig. 7(a). The exceptional reversibility and rate performance of zeolite electrodesis demonstrated by the cyclic voltammogram, which maintains its shape even at high scan rates. The hierarchical porosity of zeolite allows quick electrolyte ion transport in the material, which is attributed to the good rate capability. These CV curves have distorted rectangular shapes reflecting EDLC behavior along with some redox capacitance of zeolite[16].

3.6.3 Galvanostatic Charging-Discharging (GCD)

The GCD curves of zeolite are shown in Fig. 7(b), which supports and mimics the CV finding. The extended charge-discharge duration demonstrates the excellent capacitive characteristics of zeolite. The GCD trace of the zeolite electrode at various current densities, ranging from 0.5 to 4 Ag^{-1}, exhibits similar

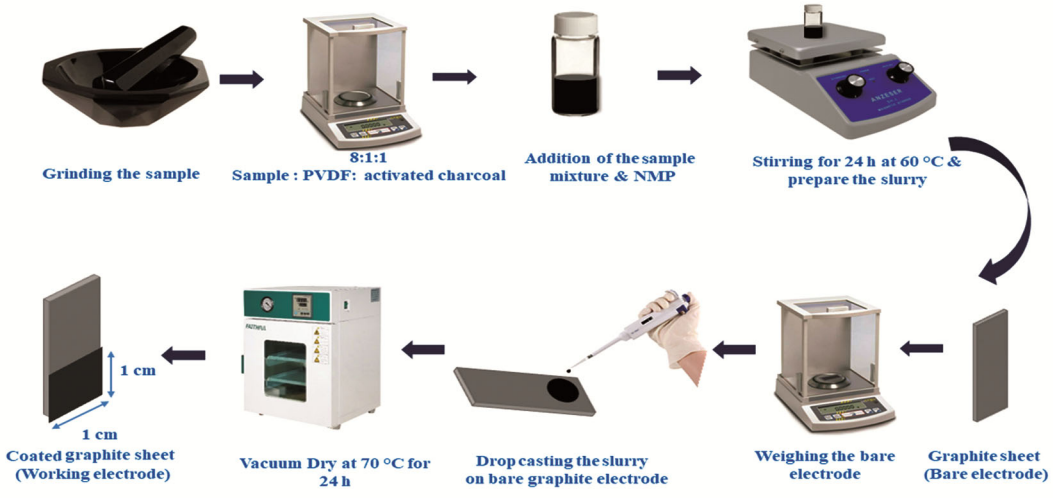

Fig. 6 — Schematic diagram for working electrode preparation.

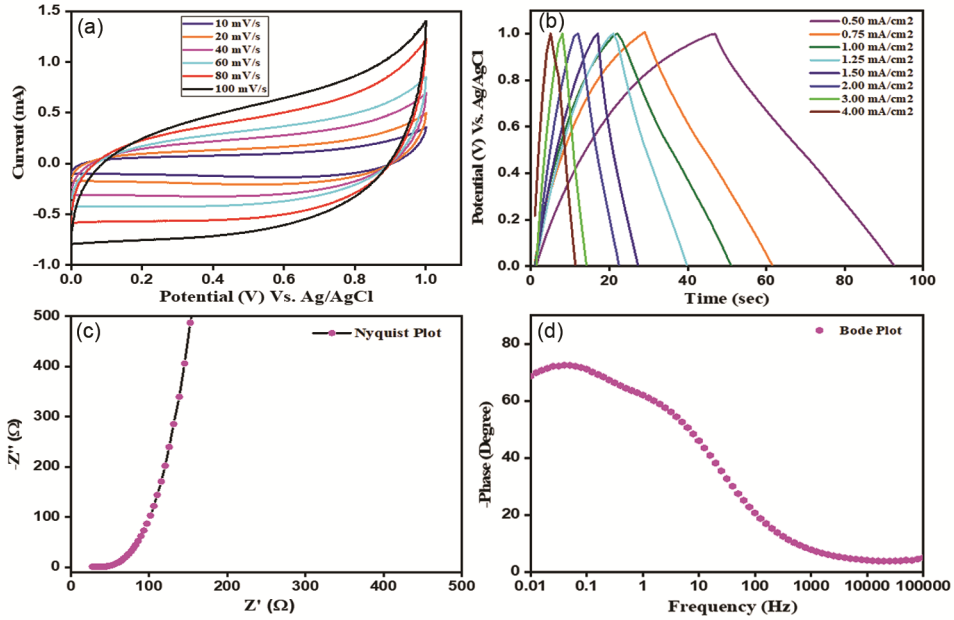

Fig. 7 — (a) CV plot of zeolite, (b) GCD profile of zeolite, (c) Nyquist plot of zeolite, and (d) Bode Plot of zeolite.

distorted triangular profiles that demonstrate the dominating EDLC nature of the fabricated electrode[17]. These almost linear GCD curves without any apparent charge-discharge voltage drop, which indicates that the electrode has a modest internal resistance[18].The specific capacitance of zeolite obtained using eq. (2) was 25, 22.5, 20, 15 and 12 Fg^{-1} at 0.5, 0.75, 1, 2, and 4 Ag^{-1} respectively.

3.6.4 Electrochemical Impedance Spectroscopy (EIS)

For exploring the internal charge transfer kinetics of the as-prepared electrode, EIS measurements of as synthesized material were performed using a perturbed signal imposed on a 5 mV bias voltage in the frequency range of 10^5 Hz to 10^{-2} Hz, and the equivalent Nyquist plots that provide relation between real and imaginary impedance are depicted in Fig. 7(c) that shows depressed semicircle in the high-frequency region and high slope straight line in the low-frequency region reflecting excellent capacitive behavior of zeolite that possess high surface area which attributes better ions diffusion pathway to deliver high capacitance value[19]. The Fig. 7(d) shows the Bode plot of zeolite that depicts excellent phase difference near about 71º which indicate the superior capacitor behavior of the material[20].

4 Conclusion

In this study, Na-P zeolite was hydrothermally synthesized from coal fly ash in alkaline medium. The characterization of the zeolite reflects successful conversion of fly ash into crystal form of Na-P zeolite. The crystallites size of as synthesized zeolite was found to be 22.3 nm along with excellent specific surface area of 118.812 m^2g^{-1}. The synthesized zeolite exhibited remarkable specific capacitance of 25 Fg^{-1} at 0.5 Ag^{-1}. Thus, this method provides a low cost and effective process for fly ash utilization into a more porous material having high surface area which can have a wide range of applications including agriculture, catalyst, energy storage, gas sensing, waste water treatment and much more.

Acknowledgments

We are grateful to IIC, IIT, Roorkee, Uttarakhand and the Department of Material Science and Engineering, NIT, Hamirpur (H.P.) for providing necessary aid for characterization tools.

References

1 Shanmugam KR, & Kulshreshtha P, *IJGEI,* 23 (2005) 15.
2 Ranjan Senapati M, *Current Sci Asso*, 100 (2011) 1791.
3 Rawat K,&Yadav AK,*Mater Today Proc*,26 (2020) 1406.
4 Paul KT, Satpathy S, Manna I, Chakraborty K, & Nando G, *Nanoscale Res Lett*,2 (2007) 397.
5 Goga F, Dudric R, Cormos C, Imre F, Bizo L, & Misca R, *Environ Eng Manag J*, 12 (2013) 337.
6 Ojha K, Pradhan NC, & Samanta AN, *Bulletin of Mater Sci*, 27(2004) 555.
7 Sangita K, Prasad B, & Udayabhanu G, *AJC*, 28(2016) 1435.

8 Pal P, Das JK, Das N, & Bandyopadhyay S, *Ultrason Sonochem* 20 (2013) 314.

9 Moafor SN, Tsobnang PK, Oyedotun KO, Lontio F R, Kabongo GL, Lebohang M, Lambi J, & Jewell L L, *RSC Adv,* 13(2023) 21393.

10 Huang S, Zhu X, Sarkar S, & Zhao Y, *APL Mater,*7 (2019) 100901.

11 Bulla M, Kumar V, Devi R, Kumar S, Sisodiya AK, Dahiya R, & Mishra A K, *Sci Rep,* 14(2024) 7389.

12 Deng L, Xu Q,&Wu H,*Procedia Environ Sci,* 31(2016) 662.

13 Musyoka NM, Petrik LF, Balfour G, Gitari WM, & Hums E, *Journal of Environmental Science and Health*, *Part A,*46 (2011) 1699.

14 Koshy N, & Singh DN, *JMCE,* 28 (2016) 04016126.

15 Kumar S, Kumar V, Bulla M, Devi R, Dahiya R, Sisodiya AK, Singh R B, & Mishra A K, *Mater Lett,* 364 (2024) 136364.

16 Zhang L, Zhao W, Jiang F, Tian M, Yang Y, Ge P, Sun W, & Ji X, *Sustain Energy Fuels,* 4(2020) 3552.

17 Ning J, Xia M, Wang D, Feng X, Zhou H, Zhang J, & Hao Y, *Nanomicro Lett, 13* (2021) 2.

18 Wang Q, Zhang Y, Jiang H, & Meng C, *J Colloid Interface Sci,*534 (2019) 142.

19 Devi R, Kumar V, Kumar S, Bulla M, & Mishra AK, *J Energy Storage,*79 (2024) 110167.

20 Zhang Y, Wang C, Dong X, Jiang H, Hu T, Meng C, & Huang C, *Chemical Engineering Journal*, 417(2021) 127964.